Fast Fourier Beamforming for Arbitrary Ultrasound Imaging Sequences Based on a K-Space Implementation of Reverse-Time Migration

Rehman Ali* and Nebojsa Duric*

*Department of Imaging Sciences, URMC, Rochester, NY, 14620 USA

ABSTRACT

The goal of Fourier beamforming is to reconstruct ultrasound images more quickly than delay-and-sum beamforming by leveraging the underlying mapping from the frequency-domain representation of the channel data to the k-space representation of the image. However, a current drawback of Fourier beamforming is its inability to generalize well to different imaging sequences. Stolt mappings have been derived for very specific imaging sequences, such as plane-wave and multistatic synthetic aperture. This work presents a generalized Stolt mapping based on reverse-time migration that can be applied to any imaging sequence. In Field II simulations of plane-wave and focused transmits, we observe that the proposed technique is comparable to REFoCUS and produces up to a 20% improvement in point target resolution compared to existing Fourier beamformers and DAS beamforming due its ability image edge waves.

Keywords: Sound speed estimation, differentiable beamforming, continuum mechanics, Lagrangian approach

1. INTRODUCTION

The goal of the Fourier beamformer is to reconstruct the ultrasound image more quickly than a delay-and-sum beamformer by leveraging underlying Stolt mappings from the frequency-domain representation of the recorded channel data to the k-space (i.e., wavenumber space) representation of the image. Early work applies Fourier beamforming to plane-wave imaging[1,2] and multistatic synthetic aperture (i.e., full-matrix capture—FMC),[3,4] each with its own set of Stolt mappings. Recent work extended the Stolt's mapping used for the multistatic setup[4] to a focused-transmit scenario[5] with the caveat that the focal depth must be the same for all transmit beams, and each transmit focus must be directly underneath a corresponding transducer element. Many conventional focused-transmit sequences fall outside this limited use case. Because different imaging sequences require different Stolt mappings,[1,5] and in many cases, a closed-form Stolt mapping may not be known, Fourier beamforming is often restricted to a limited set of use cases.

Fourier beamforming currently lacks a unifying framework that applies to all transmit sequences. Retrospective encoding for conventional ultrasound sequences (REFoCUS) [5][6,7] could be applied to any transmit sequence to recover multistatic data, which has a known Stolt mapping;[4] however, if the imaging sequence has far fewer transmit events than number of elements (e.g., 15 plane waves from a 128-element array), conversion to multistatic data will increase computational cost. A generalized Fourier beamformer should be applicable to any transmit sequence without first converting to a multistatic representation. Because reverse-time migration (RTM) generalizes to all transmit sequences without requiring an intermediate multistatic representation,[8] we present a generalized Stolt mapping based on a k-space representation of RTM.

Further author information: (Send correspondence to Rehman Ali)
Rehman Ali: E-mail: Rehman$_{A}li@URMC.Rochester.edu$

Medical Imaging 2026: Ultrasonic Imaging and Tomography, edited by Christian Boehm, Mohammad Mehrmohammadi, Shawn Liangzhong Xiang, Proc. of SPIE Vol. 13931, 139311M · 2026 Published by SPIE
1605-7422 · doi: 10.1117/12.3085601

2. BACKGROUND AND THEORY

2.1 Reverse-Time Migration: Cross-Correlation of Transmit and Receive Wavefields

Pulse-echo ultrasound images can be created by propagating transmit and receive wavefields $p_{tx(i)}(x,z,t)$ and $p_{rx(i)}(x,z,t)$ based on the transmit sequence and receive channel data collected from each transmit event $i = 1, ..., N_{tx}$. Partial images $I_i(x,z)$ prior to amplitude detection can be formed by the following cross-correlation:

$$I_i(x,z) = \int_0^\infty p^*_{tx(i)}(x,z,t)p_{rx(i)}(x,z,t)dt = \int_0^\infty p^*_{tx(i)}(x,z,f)p_{rx(i)}(x,z,f)df. \tag{1}$$

2.2 Calculating Transmit and Receive Wavefields via the Angular Spectrum Method

The frequency-domain transmit $p_{tx(i)}(x,z,f)$ and receive $p_{rx(i)}(x,z,f)$ wavefields are calculated according to

$$p_{tx(i)}(k_x,z,f) = \hat{p}_{tx(i)}(k_x,f)e^{-j2\pi(k^2-k_x^2)^{1/2}z}, \tag{2}$$

$$p_{rx(i)}(k_x,z,f) = \hat{p}_{rx(i)}(k_x,f)e^{+j2\pi(k^2-k_x^2)^{1/2}z}. \tag{3}$$

where k_x is the Fourier-transform-coordinate or wavenumber-space dual corresponding to lateral coordinate x, $\hat{p}_{tx(i)}(k_x,f) = p_{tx(i)}(k_x,z=0,f)$ and $\hat{p}_{rx(i)}(k_x,f) = p_{rx(i)}(k_x,z=0,f)$ represent the frequency spectra of the transmit pulse and receive channel data from each element on the array (located at $z=0$), and $k = \frac{f}{c}$ for sound speed c and frequency f. Knowledge of the transmit pulse spectrum $P(f)$, transmit focal delays $\tau_i(x)$, and transmit apodization $A_i(x)$ for each transmit event i is used to form $\hat{p}_{tx(i)}(x,f)$:[8]

$$\hat{p}_{tx(i)}(x,f) = A_i(x)P(f)e^{-j2\pi f\tau_i(x)}. \tag{4}$$

2.3 Deriving the K-Space Representation of Reverse-Time Migration via Stolt Mapping

The following inverse Fourier transforms are defined on transmit and receive, respectively:

$$p_{tx(i)}(x,z,f) = \int_{-\infty}^\infty p_{tx(i)}(k_x^{tx},z,f)e^{+j2\pi k_x^{tx}x}dk_x^{tx}, \tag{5}$$

$$p_{rx(i)}(x,z,f) = \int_{-\infty}^\infty p_{rx(i)}(k_x^{rx},z,f)e^{+j2\pi k_x^{rx}x}dk_x^{rx}. \tag{6}$$

The body of the integral over frequency in equation (1) can then be written as:

$$p^*_{tx(i)}(x,z,f)p_{rx(i)}(x,z,f) = \int_{-\infty}^\infty\int_{-\infty}^\infty p^*_{tx(i)}(k_x^{tx},z,f)p_{rx(i)}(k_x^{rx},z,f)e^{+j2\pi(k_x^{rx}-k_x^{tx})x}dk_x^{rx}dk_x^{tx}. \tag{7}$$

If we substitute $k_x^{rx} = k_x^{tx} + k_x$, equation (7) can be written as

$$p^*_{tx(i)}(x,z,f)p_{rx(i)}(x,z,f) = \int_{-\infty}^\infty C_i(k_x,z,f)e^{+j2\pi k_x x}dk_x, \tag{8}$$

$$C_i(k_x,z,f) = \int_{-\infty}^\infty p^*_{tx(i)}(k_x^{tx},z,f)p_{rx(i)}(k_x^{tx}+k_x,z,f)dk_x^{tx}, \tag{9}$$

which implies the following about the k-space $I_i(k_x,k_z)$ of the image $I_i(x,z)$:

$$I_i(x,z) = \int_0^\infty p^*_{tx(i)}(x,z,f)p_{rx(i)}(x,z,f)df = \int_0^\infty\int_{-\infty}^\infty C_i(k_x,z,f)e^{+j2\pi k_x x}dk_x df, \tag{10}$$

$$I_i(x,z) = \int_0^\infty\int_{-\infty}^\infty\int_{-\infty}^\infty C_i(k_x,k_z,f)e^{+j2\pi k_x x}e^{+j2\pi k_z z}dk_x dk_z df. \tag{11}$$

$$I_i(k_x, k_z) = \int_0^{\infty} C_i(k_x, k_z, f) e^{+j2\pi k_x x} e^{+j2\pi k_z z} df. \tag{12}$$

Substituting equations (2) and (3) into equation (9) yields

$$C_i(k_x, z, f) = \int_{-\infty}^{\infty} \hat{p}^*_{tx(i)}(k_x^{tx}, f) \hat{p}_{rx(i)}(k_x^{tx} + k_x, f) e^{+j2\pi\left[(k^2-(k_x^{tx})^2)^{1/2} + (k^2-(k_x^{tx}+k_x)^2)^{1/2}\right]z} dk_x^{tx}, \tag{13}$$

$$C_i(k_x, k_z, f) = \int_{-\infty}^{\infty} \hat{p}^*_{tx(i)}(k_x^{tx}, f) \hat{p}_{rx(i)}(k_x^{tx} + k_x, f) \delta(k_z - [k^2 - (k_x^{tx})^2]^{1/2} - [k^2 - (k_x^{tx} + k_x)^2]^{1/2}) dk_x^{tx}. \tag{14}$$

2.4 Forward and Inverse Stolt Mapping for Reverse-Time Migration

The integration over f in equation (12) evaluates the delta function $\delta(\cdot)$ in equation (14). Therefore, the forward Stolt mapping from k to k_z is determined by setting the argument of $\delta(\cdot)$ to 0:

$$k_z = (k^2 - (k_x^{tx})^2)^{1/2} + (k^2 - (k_x^{tx} + k_x)^2)^{1/2} \tag{15}$$

The inverse Stolt mapping (from k to k_z) needed to calculate $I_i(k_x, k_z)$ is

$$k = \frac{\left(4k_x^{tx}(k_x^{tx} + k_x)(k_x^2 + k_z^2) + (k_x^2 + k_z^2)^2\right)^{1/2}}{2k_z}. \tag{16}$$

Finally, the full k-space $I_i(k_x, k_z)$ of the image $I_i(x, z)$ can be calculated (recall that $f = ck$):

$$I_i(k_x, k_z) = \int_{-\infty}^{\infty} \hat{C}_i\left(k_x^{tx}, k_x, f = \frac{c}{2k_z}\left(4k_x^{tx}(k_x^{tx} + k_x)(k_x^2 + k_z^2) + (k_x^2 + k_z^2)^2\right)^{1/2}\right) dk_x^{tx}. \tag{17}$$

$$\hat{C}_i(k_x^{tx}, k_x, f) = \hat{p}^*_{tx(i)}(k_x^{tx}, f) \hat{p}_{rx(i)}(k_x^{tx} + k_x, f) \tag{18}$$

3. METHODS

Field II[9,10] simulations of radio-frequency channel data for multistatic synthetic aperture, plane-wave, and walking-aperture focused transmit sequences with the same acquisition parameter described in the prior work on RTM[8] were used to compare delay-and-sum (DAS) beamforming,[11] the previous Fourier beamformers,[1,4,5] a multistatic FMC Stolt migration[4] after REFoCUS,[7,12] and the RTM-based Fourier beamformer proposed in this work. For plane-wave imaging we found that Lu's method[1] generally provided better resolution and contrast than Garcia's method[2] and became the Fourier beamformer used for comparison. For focused transmit imaging, the modified FMC Stolt migration for fixed focal depth imaging[5] became the basis for comparison. In each case, we measure the lateral full-width at half-maximum (FWHM) point target resolution at 35 mm.

4. RESULTS AND DISCUSSION

Figure 1 compares our proposed RTM-based Stolt migration to DAS beamforming (based on virtual source synthetic aperture[11]), the previous Fourier beamformers,[1,4,5] and FMC Stolt migration[4] applied to multistatic data recovered by REFoCUS.[7,12] In the multistatic imaging case, REFoCUS is not used because we are already working with multistatic data; therefore, the 2nd and 3rd column of Figure 1 are identical for the multistatic imaging case. There is a very small improvement in the FWHM resolution from 0.27 to 0.26 to 0.25 mm when going from the DAS beamformer to multistatic Stolt migration[4] to our proposed RTM-based Stolt mapping. In theory, the FWHM resolution of multistatic imaging should be identical for all 3 imaging methods. In the plane-wave imaging case, the FWHM resolution improves from 0.35 to 0.34 to 0.28 to 0.27 mm with the 2nd column corresponding to Lu's Fourier beamformer.[1] In the focused transmit case, the FWHM resolution improves from 0.46 to 0.38 to 0.35 to 0.35 mm with the 2nd column representing focused-transmit FMC Stolt migration.[5] In both the plane-wave and focused-transmit imaging cases, the improvement from the first two methods to the last two methods can be attributed to edge waves[6] produced by each set of transmits.

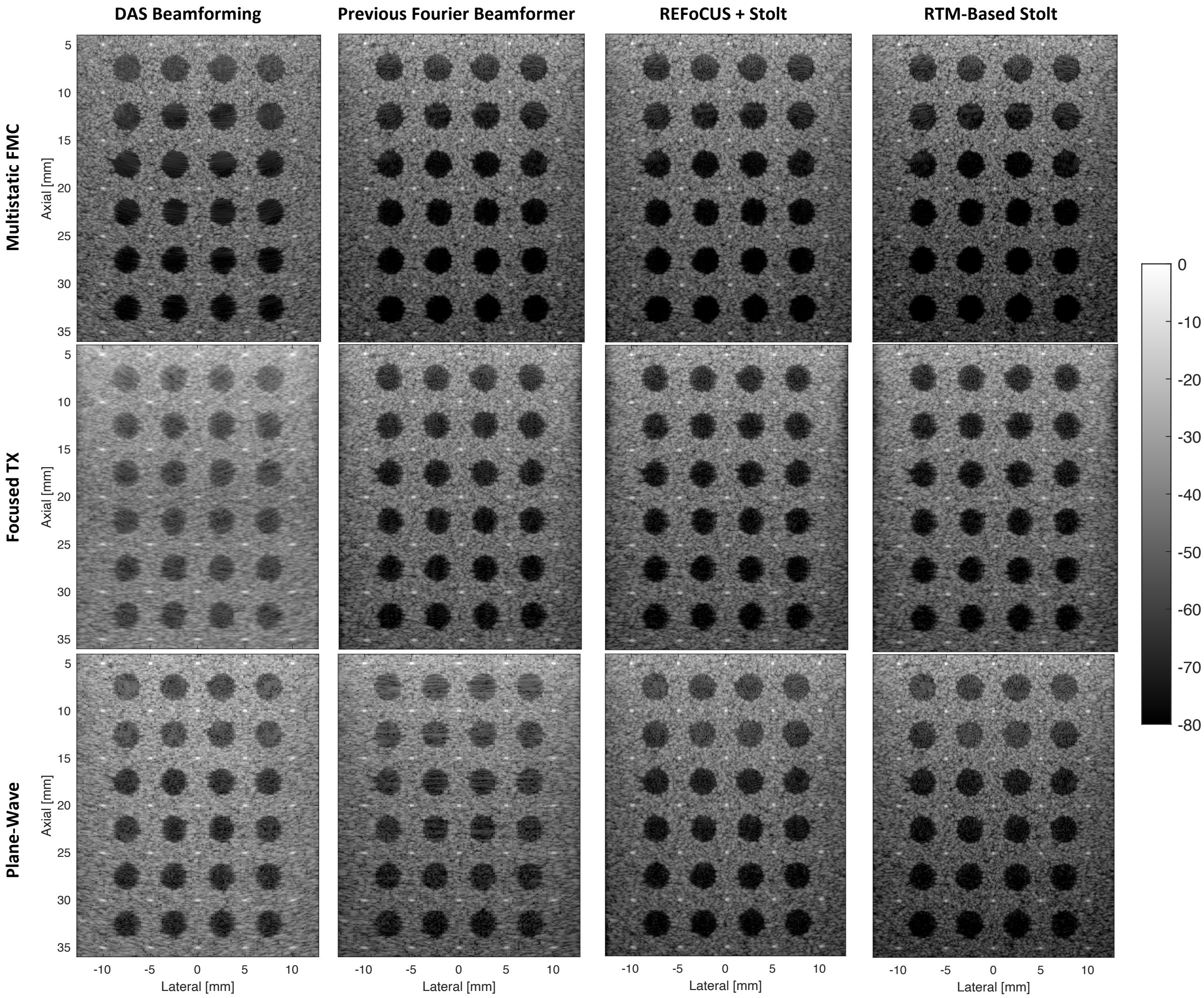

Figure 1. Comparison of RTM-based Stolt mapping to DAS beamforming, the previous Fourier beamformers,[1,4,5] and REFoCUS[7,12] followed by the full multistatic Stolt mapping[4] after recovering the full multistatic dataset.

These results show that both REFoCUS followed by FMC Stolt migration and the proposed RTM-based Stolt migration generalize well across imaging sequences. Generally, the proposed RTM-based Stolt migration is slower than simply applying REFoCUS prior to FMC Stolt migration. However, the RTM-based Stolt migration offers the flexibility of reconstructing images from individual transmit events, which may be useful for coherence imaging.[13–15] While the relative benefits of REFoCUS followed by FMC Stolt migration and the RTM-based approach requires further study, this work aims to connect RTM to the broader family of Fourier beamformers and provide an open-source implementation.

A key motivation for this work was to provide an open-source repository where all the Fourier beamformers, including the RTM-based approach proposed here, would be implemented. One of the challenges associated with the broader adoption of these Fourier beamforming techniques was the lack of publicly available code and the difficulties associated with connecting the underlying mathematical concepts to a practical implementation. The prior work that made f-k Stolt migration[2] open-source started the path towards a practical implementation that was broadly accessible and well-understood. However, the implementations of several previous Fourier beamformers[1,4] had not been made public. An interesting result from the prior work[2] was that Lu's method[1] better replicated DAS beamforming; despite this, Garcia's method[2] become more popular, likely due to the availablity of an open-source code. Therefore, the broader goal of this work is not to assert the benefits of any specific approach but to enable a more objective comparison across Fourier beamformers while connecting the mathematical theory to practical implementation.

5. CONCLUSIONS

We present an RTM-based Stolt mapping that generalize Fourier beamforming to any transmit sequence and provides comparable resolution and image quality to the FMC Stolt migration applied to multistatic dataset recovered by REFoCUS. When compared to previous Fourier beamformers and DAS, REFoCUS and the RTM-based Fourier beamformer appear to provide superior image resolution due to their ability to image edge waves. To facilitate comparison of the RTM-based Fourier beamformer with the other Fourier beamformers described, open-source implementations of each Fourier beamformer has been provided: https://github.com/rehmanali1994/FastFourierBeamformers.

ACKNOWLEDGMENTS

This work was supported by the National Institute of Biomedical Imaging and Bioengineering (NIBIB) from the National Institute of Health (NIH) under grants F32-EB034589 and K99-EB037080.

REFERENCES

[1] Cheng, J. and Lu, J.-y., "Extended high-frame rate imaging method with limited-diffraction beams," *IEEE transactions on ultrasonics, ferroelectrics, and frequency control* **53**(5), 880–899 (2006).

[2] Garcia, D., Le Tarnec, L., Muth, S., Montagnon, E., Porée, J., and Cloutier, G., "Stolt's fk migration for plane wave ultrasound imaging," *IEEE transactions on ultrasonics, ferroelectrics, and frequency control* **60**(9), 1853–1867 (2013).

[3] Ylitalo, J. T. and Ermert, H., "Ultrasound synthetic aperture imaging: monostatic approach," *IEEE transactions on ultrasonics, ferroelectrics, and frequency control* **41**(3), 333–339 (2002).

[4] Hunter, A. J., Drinkwater, B. W., and Wilcox, P. D., "The wavenumber algorithm for full-matrix imaging using an ultrasonic array," *IEEE transactions on ultrasonics, ferroelectrics, and frequency control* **55**(11), 2450–2462 (2008).

[5] Jiang, C., Liu, C., Zhan, Y., and Ta, D., "The spectrum-beamformer for conventional b-mode ultrasound imaging system: principle, validation, and robustness," *Ultrasonic Imaging* **44**(2-3), 59–76 (2022).

[6] Bottenus, N., "A method for intrapulse spatial compounding," in [*2016 IEEE International Ultrasonics Symposium (IUS)*], 1–4, IEEE (2016).

[7] Ali, R., Herickhoff, C. D., Hyun, D., Dahl, J. J., and Bottenus, N., "Extending retrospective encoding for robust recovery of the multistatic data set," *IEEE transactions on ultrasonics, ferroelectrics, and frequency control* **67**(5), 943–956 (2019).

[8] Ali, R., "Fourier-based synthetic-aperture imaging for arbitrary transmissions by cross-correlation of transmitted and received wave-fields," *Ultrasonic imaging* **43**(5), 282–294 (2021).

[9] Jensen, J. A. and Svendsen, N. B., "Calculation of pressure fields from arbitrarily shaped, apodized, and excited ultrasound transducers," *IEEE transactions on ultrasonics, ferroelectrics, and frequency control* **39**(2), 262–267 (1992).

[10] Jensen, J. A., "Field: A program for simulating ultrasound systems," *Medical & Biological Engineering & Computing* **34**(sup. 1), 351–353 (1997).

[11] Bae, M.-H. and Jeong, M.-K., "A study of synthetic-aperture imaging with virtual source elements in b-mode ultrasound imaging systems," *IEEE transactions on ultrasonics, ferroelectrics, and frequency control* **47**(6), 1510–1519 (2000).

[12] Bottenus, N., "Recovery of the complete data set from focused transmit beams," *IEEE transactions on ultrasonics, ferroelectrics, and frequency control* **65**(1), 30–38 (2017).

[13] Bell, M. A. L., Goswami, R., Kisslo, J. A., Dahl, J. J., and Trahey, G. E., "Short-lag spatial coherence imaging of cardiac ultrasound data: Initial clinical results," *Ultrasound in medicine & biology* **39**(10), 1861–1874 (2013).

[14] Li, Y. L. and Dahl, J. J., "Angular coherence in ultrasound imaging: Theory and applications," *The Journal of the Acoustical Society of America* **141**(3), 1582–1594 (2017).
[15] Li, P.-C. and Li, M.-L., "Adaptive imaging using the generalized coherence factor," *IEEE transactions on ultrasonics, ferroelectrics, and frequency control* **50**(2), 128–141 (2003).